Spin resonance of electrons localized on Ge/Si quantum dots

A. F. Zinovieva,* A. V. Dvurechenskii, N. P. Stepina, A. S. Deryabin, and A. I. Nikiforov
Institute of Semiconductor Physics, 630090 Novosibirsk, Russia

R. M. Rubinger,† N. A. Sobolev, J. P. Leitão, and M. C. Carmo
Departamento de Fisica e I3N, Universidade de Aveiro, Aveiro 3810-193, Portugal

Spin resonance of electron states in a Ge/Si heterosystem with Ge quantum dots has been investigated. Electron localization in the strain-induced potential wells in Si in the vicinity of the Ge dots is confirmed by an analysis of the obtained g-tensor values. A well pronounced anisotropy of the linewidth is explained in terms of an effective magnetic field, lying in the plane of the quantum dot array. This magnetic field arises during the tunneling of electrons between quantum dots and leads to an acceleration of the spin relaxation. The origin of the field is the structure-induced asymmetry of electron potential wells. Two ways of increasing the spin lifetime are suggested: (1) the creation of a higher symmetry confinement potential for electrons and (2) the growth of a well-separated quantum dot array.

PACS number(s): 73.21.La, 03.67.Lx, 72.25.Rb

I. INTRODUCTION

The electron spin can be considered as a natural bit of quantum information and can provide an implementation of the ideas of quantum computation.[1] Strong confinement in low-dimensional structures such as quantum wells (QWs) and quantum dots (QDs) leads to a significant increase of spin lifetimes.[2] An extremely long spin lifetime is expected in zero-dimensional structures based on Si due to weak spin-orbit (SO) coupling in this material. A promising way for the creation of zero-dimensional structures is the strain epitaxy. Semiconductor QDs fabricated by this technique can be controllably positioned, electronically coupled, and embedded into active devices. The Ge/Si heterosystem is one of the most suitable systems for strong electron confinement in all three dimensions in Si. Ge layers can serve as barriers limiting electron movement in the Z direction and the electrons can be easily localized in the strained Si layer between them. The localization in the X and Y directions can be reached through a strain modulation in the Si layer. An interchange of local compression and tension modulates the conduction band edge and results in the appearance of a three-dimensional potential well. Ge QDs introduced as sources of inhomogeneous strain can be centers of electron localization. The strain is maximum near the apex of a Ge QD and decays in Si, thus forming a triangular potential well for the electrons.

A three-dimensional view of a potential well for electrons emerging due to the strain in Si nearby a Ge QD is shown in Fig. 1. This image reflects the result of strain calculations for a typical Ge/Si quantum dot (lateral size $l=15$ nm and height $h=1.5$ nm) using a Keating interatomic potential. As one can see, the potential well for electrons is formed near the apex and under the bottom of the dot. According to calculations in the effective mass approximation, the electron ground state is confined near the apex of the QD with binding energy $E_0 \approx 10$ meV, while the first excited state is located under the bottom of the QD and has binding energy $E_1 \approx 8$ meV. Values of deformation potentials and band offsets for Ge/Si system used in the calculations were taken from Ref. 3.

For a successful manipulation of spins in QDs, it is necessary to know such fundamental spin properties as the effective g factor that defines the Zeeman splitting and the spin relaxation time. These values are usually obtained from electron spin resonance (ESR) measurements. A commonly used opinion is that the size dispersion of self-assembled QDs leads to a broadening of the ESR line and makes direct ESR observations impossible. Recently, attempts to measure ESR on Ge QD arrays grown on prepatterned substrates have been undertaken.[4] For comparison with the ordered QD arrays, the authors[4] also studied ESR signal from the self-assembled QDs. Under illumination with sub-band-gap light, the prepatterned samples exhibited ESR signals with a g factor close to that of the conduction electrons in Si, $g=1.998$, with an isotropic angular dependence. The last feature suggests that the observed signal belongs more likely to nonlocalized elec-
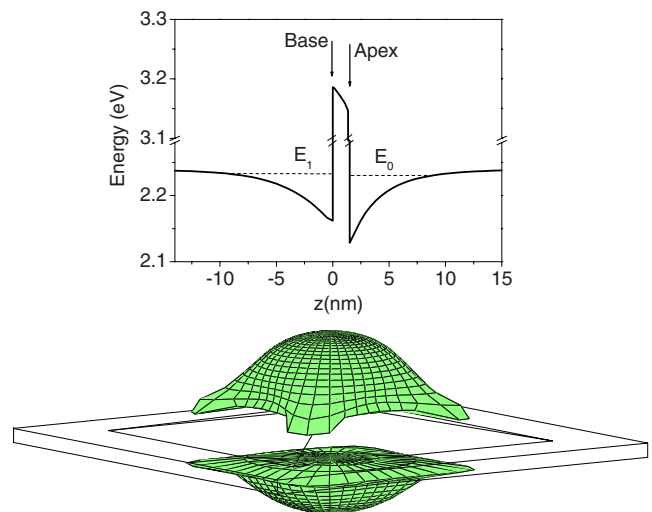

FIG. 1. (Color online) Electron potential isosurfaces near a Ge dot for $U=-0.03$ eV with respect to the conduction band edge of unstrained Si. In the upper panel, a potential profile along the z direction is shown. The energies of ground and first excited states are indicated as E_0 and E_1, respectively.
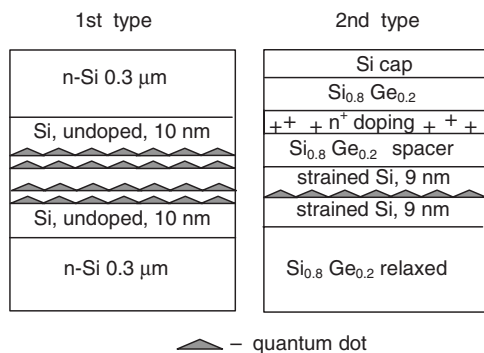
FIG. 2. The structure of the samples.

trons than to electrons bound to QDs. The statement is also supported by unusually short ($T_1, T_2 \sim 1$ μs) spin relaxation times measured in this system. Times of this order of magnitude are typical of the electron spin relaxation in two-dimensional (2D) asymmetrical structures,[5] but not of localized electron states in Si. However, the self-assembled array with a higher density of QDs produced a more intense signal than the prepatterned sample. This argues in favor of signal origin from the electrons localized on the QDs. From this point of view, the question on the relation of the observed signal to the electrons localized on QDs has to be clarified.

In the present work, we have performed ESR measurements on Ge/Si heterostructures with self-assembled QDs and adduce direct evidence that the observed ESR signal stems from the electrons localized in the vicinity of the Ge QDs. We demonstrate that the QD size dispersion has no significance for electrons in the Ge/Si QD heterostructure in contrast to other semiconductor systems with a stronger SO interaction. It has been shown that in the Ge/Si QD structures, the strain has a crucial effect on the g factor of the localized electrons. On the contrary, the electron binding energy plays a negligible role.

II. SAMPLES AND EXPERIMENT

Two type of structures with self-assembled Ge QDs were prepared for the ESR measurements: (1) a four-layer stacked QD structure and (2) a SiGe/Si/SiGe QW structure with a QD layer embedded in the middle of a strained Si channel. The QD structure was optimized with the aim to enlarge the electron binding energy E_b in the Si potential well near a QD, as E_b in a sample with a single Ge QD layer is very small (see Fig. 1). One way to enlarge E_b is the growth of a vertical stack of Ge islands. The accumulation of the strain from different QD layers in the stack leads to an increase of the potential well depth. A second way to confine electrons is embedding of a Ge QD layer in the middle of a strained Si channel in a SiGe/Si/SiGe QW structure. In this case, the strain in the Si channel together with the local strain around Ge QDs leads to a stronger electron confinement.

The samples were grown by molecular-beam epitaxy on n-Si(001) substrates with a resistivity of 1000 Ω cm. The layer sequences and their parameters are shown in Fig. 2. The density of QDs is $\sim 10^{11}$ cm^{-2} in both structures. Scan-

ning tunneling microscopy of a sample without the Si capping layer showed that the Ge islands have a shape of "hut" clusters with the average lateral size $l=20$ nm and height $h=2$ nm. The growth temperature of the fourfold stack structure was 500 °C. Four layers of Ge islands were inserted in the middle of a 0.6 μm epitaxial n-Si layer (Sb concentration $n \sim 5 \times 10^{16}$ cm^{-3}). In order to reduce the distortion of the electron confining potential by the potential of ionized impurities, 10 nm thick undoped Si spacer layers were introduced between the stack of Ge QDs and the n-type Si layers. The first and second Ge layers as well as the third and fourth ones are separated by 3 nm thick Si spacers, while the distance between the second and third Ge layers is 5 nm. According to the numerical calculations using the effective-mass approximation,[6] the electron localization occurs between the second and third QD layers at the apices of the Ge dots, and the electron binding energy amounts to 60 meV.

The SiGe/Si/SiGe QW structure containing QDs was grown on a 0.5 μm strain-relaxed Si$_{0.8}$Ge$_{0.2}$ buffer layer, followed by a Si QW, modulation doped Si$_{0.8}$Ge$_{0.2}$ layers, and a Si cap. According to the x-ray diffractometry data, the relaxation degree of the SiGe buffer layer is 58.8%. This leads to a lower than expected E_c band offset at the Si/Si$_{0.8}$Ge$_{0.2}$ interface (≈ 60 meV instead of ≈ 100 meV) for a fully relaxed SiGe buffer layer.[7] The incorporation of Ge QDs into the strained Si layer provokes the formation of additional local strain fields in Si around the Ge QDs. Within the scope of the linear elasticity theory, we can describe the resulting strain field as a linear superposition of a local strain field produced by a QD and a uniform strain in the Si layer. To find the local strain near the QD, we can neglect the presence of the Si/SiGe interfaces and use the solution for QD incorporated in an infinite matrix. We introduce the uniform strain as a change of the matrix lattice constant. This solution gives the binding energy $E_b \approx 10$ meV with respect to the conduction band edge of the Si channel. Combining this result with the band offset at the Si/SiGe boundaries, we obtain the resulting E_b value. This estimate gives the binding energy $E_b \approx 70$ meV.

We measured the ESR using a standard Bruker X-band spectrometer operating at a frequency close to 9.38 GHz at sample temperatures ranging from 3.9 to 20 K.

III. RESULTS AND DISCUSSION

A. Electron spin resonance signal

Both QD structures show similar ESR signals that we attribute to electrons localized in the Si potential wells near the apices of the Ge dots (Fig. 3). The observed ESR line exhibits an inhomogeneous broadening. The linewidth ΔH_{pp} is about 0.8 Oe for the magnetic field $\mathbf{H} \| Z$, where Z is the [001] growth direction of the structure. Upon deviation of the magnetic field from the Z axis, the ESR line becomes broader and weaker. For the in-plane magnetic field $\mathbf{H} \perp Z$, the linewidth ΔH_{pp} is approximately four times larger than ΔH_{pp} for $\mathbf{H} \| Z$. The g tensor is axially symmetric with the principal values $g_{zz} = 1.9995 \pm 0.0001$ and $g_{xx} = g_{yy} = 1.9984 \pm 0.0001$. The difference between the g factors in the first and second structures is $\Delta g \approx 0.0001$ and lies within
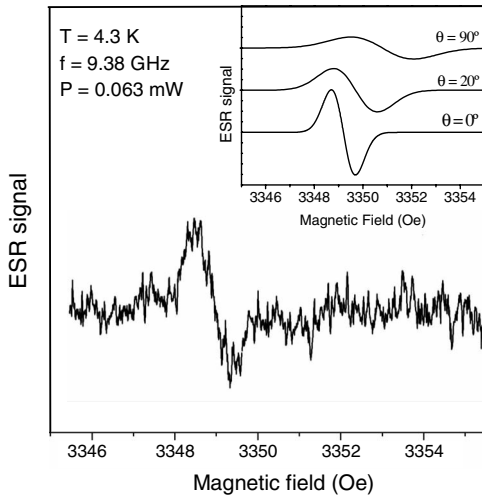
FIG. 3. ESR signal of electrons localized on Ge/Si QDs in the fourfold stack structure. The inset shows the linewidth variation vs orientation of the external magnetic field. The shift of the ESR line comes from the anisotropy of the g factor. The noise has been removed by numerical treatment.

the accuracy limits of our measurements. The angular dependence of the g factor is described by $g = [g_{zz}^2 \cos^2(\theta) + g_{xx}^2 \sin^2(\theta)]^{1/2}$, where θ is the angle between the magnetic field and the Z axis (Fig. 4).

Foremost, we present a proof that the electrons localized on the Ge QDs are responsible for the observed ESR signal. These are the following testimonies for this statement: (1) such a type of signal has not been observed in the reference structures without QDs; (2) the principal g-tensor values exactly coincide with the longitudinal and transversal components of the electron g tensor in bulk Si ($g_{zz} = g_\parallel = 1.9995$ and $g_{xx} = g_{yy} = g_\perp = 1.9984$), and the obtained g factor is anisotropic. This behavior is typical of localized electrons in uniaxially strained Si regions.
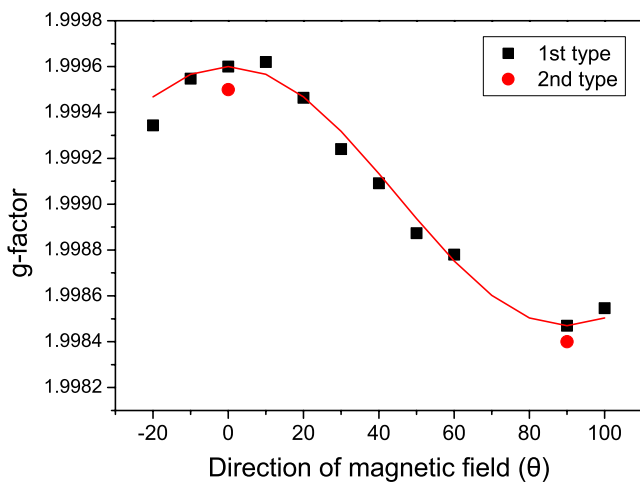

FIG. 4. (Color online) Angular dependence of the electron g factor. For $\Theta = 0$, the magnetic field is parallel to the growth direction of the structure.

B. Strain effect

In the Si region adjacent to the Ge QD apex, the strain distribution is close to the following one: an effective uniaxial compression along the growth direction of structure Z and an in-plane tension. These strains cause a splitting of the sixfold-degenerate Δ valley and a separation of the two lower Δ valleys along the [001] growth direction and of the four upper in-plane Δ valleys. The conduction band edge is formed by the two lower Δ valleys. Therefore, the symmetry of the g tensor is the same as that of the isoenergetic surface (a rotational ellipsoid). When the external magnetic field **H** is applied parallel to the ellipsoid axis, we observed the pure $g_\parallel$ value, and when **H** is perpendicular to this axis, $g_\perp$ is measured.

The electron state in nonstrained bulk Si is built from the wave functions of all six ellipsoids at the Δ point, and the effective g factor is given by mixing: $\frac{1}{3}g_\parallel + \frac{2}{3}g_\perp = 1.9987$.[8] In our case, no mixing of ellipsoids occurs due to the splitting of the Δ valley. The magnitude of this splitting depends on the biaxial strain ($\varepsilon_{zz} - \varepsilon_{xx}$).[9] A decrease of the biaxial strain can cause a narrowing of the energy gap between the Δ valleys, and as a consequence, an increased admixture of the upper Δ-valley states into the electron state. This can cause an effective change of the g factor. This approach allows explaining the value of g factor equal to 1.998, formerly obtained in the experiments with stacks of 12 Ge QD layers.[4] In these experiments, the Ge QD layers were separated by 25 nm thick Si spacers. This distance is too long for a strain accumulation from different QD layers to be efficient. Strain in this structure is not sufficient for any noticeable splitting of the Δ valleys and, therefore, the g factor of the electron states on Ge QDs only slightly differs from that of the electron states in the bulk nonstrained Si. Thus, the strain in Si near a Ge QD apex strongly affects the magnitude of the g factor. It should be noted that the value of biaxial strain is practically the same for all QDs in the array, because it is determined by the aspect ratio h/l. This very fact provides a chance to observe the ESR signal of electrons on Ge QDs.

C. Size dispersion effect

At first glance, the inhomogeneous broadening of the ESR line can be explained by the size dispersion of QDs. The latter provides some variation of electron binding energies in QD array. In our samples, the size dispersion of quantum dots is about ~10%, which leads to a binding energy variation of a few meV. The difference between the binding energies in the two types of investigated structures is 10 meV. This is the upper limit of the energy discrepancy in our samples. Our experimental results demonstrate that such a difference does not lead to any significant change of the g-factor values: in both structures, we obtain practically identical g factors. The same conclusion can be drawn from the following simple reasoning. The g-factor value can be estimated from the equation $\delta g = g - g_0 \approx \lambda / \Delta E$, where g_0 is the free electron g factor, λ is the SO interaction constant, and ΔE is the energy gap between the electron level and the nearest energy band. In Si, $\lambda \approx 44$ meV and $\Delta E \approx 4$ eV.[10] The change of ΔE by 10 meV has no noticeable effect on the g factor.

However, it is noteworthy that in the case of traditional donors in Si (P, Sb, and As), the strong dependence of the *g*-factor value on the electron binding energy is well known. For example, a difference of 10 meV in the binding energy of Sb and As leads to a *g*-factor shift of 2.1×10^{-4}.[11] The origin of this effect is the dependence of the hyperfine interaction constants $a \sim \psi^2$ on the type of donor nucleus. For a higher binding energy, the constant *a* is larger. The relationship between the *g* factor and the constant *a* is defined by the Breit-Rabi equation,[12] and was experimentally detected for donors in Si by Feher.[11] In our samples, the QDs and surrounding Si were undoped, and the electron localization on the QDs is caused by strain rather than by Coulomb interaction with ionized donors. The absence of donor nucleus in the electron localization area provides the independence of the *g*-factor value of the binding energy.

D. Ge/Si mixing effect

Besides the strain, there is another important parameter affecting the electron *g*-factor value. This is the wave function penetration under Ge barrier that limits the electron movement in the *Z* direction. The SO interaction in Ge is by an order of magnitude stronger than in Si, and the *g* factor can significantly depend on the degree of penetration. The barrier height can be lower due to a Ge/Si intermixing during the growth, which can bring about deviations of the *g* factors in structures grown at different temperatures. In our samples, the *g*-factor values are practically equal, although in the first type of structure, the mixing of Ge and Si inside the QDs is stronger (the growth temperature is higher). Below we find the reason for the small difference between the *g* factors in the two types of investigated structures.

The *g* factor of an electron state localized at the Si/SiGe interface is given by

$$g_{el} = \alpha g_{Si} + \beta g_{SiGe},$$

where α is the part of the wave function inside the Si potential well, and $\beta = 1 - \alpha$ is the part of the wave function penetrating the SiGe barrier.

To use this equation in calculations, one needs the value of g_{SiGe}, and in the case of pure Ge QDs, g_{Ge} is required. The conduction band minimum in Ge lies in the *L* valley. Therefore, the experimental and theoretical *g*-factor values have been obtained for this valley.[8] In Si, the conduction band minimum lies in the Δ valley. The tails of electron wave function penetrating the Si/Ge barrier will also belong to the Δ valley in the Ge region, because for a transition to the *L* valley, the electron must suffer scattering with a too large change of the momentum *k*. However, there is no available information about the *g*-factor value for the Δ valley in Ge. Following the approach proposed by Liu,[13] we are going to obtain the theoretical *g*-factor values in the Δ valley of Ge. We take into account not only the nearest valence bands, but also the interaction with deep-lying 3*p* states. Liu has obtained a good quantitative agreement between the measured and calculated *g*-factor values for the Δ valley in Si. Using the similarity of the Si and Ge energy band structures near the Δ point, we obtain the contribution to the *g*-factor value
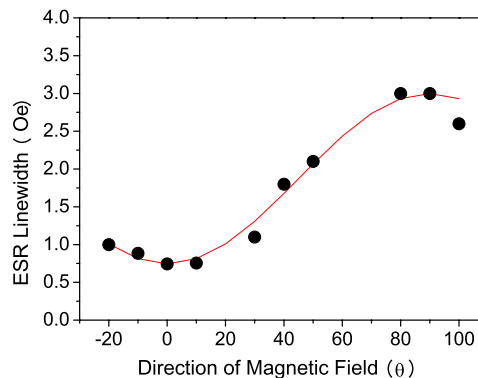

FIG. 5. (Color online) Angular dependence of the ESR linewidth upon sample rotation around a [011] axis. For $\Theta = 0$, the applied magnetic field is parallel to the growth direction of the structure. The circles are experimental data. The solid line is the theoretical approximation.

from the core states. For the calculation of the contribution of the nearest bands, we take the **kp** method described by Cardona and Pollak.[14] Summing up these contributions, we obtain the theoretical *g*-factor values in the Δ valley of Ge: $g_\parallel^{Ge\Delta} = 2.0412$ and $g_\perp^{Ge\Delta} = 1.8873$. Using these values, one can calculate the electron *g* factor in any SiGe nanostructure with a Si-like conduction band, where the band minimum lies in the Δ valley.

Turning back to our experiments and taking into account the analysis of Raman measurements made in Ref. 6, we conclude that the mixing of Ge and Si in the fourfold stack QD structure leads to a lower Ge content (~ 0.7) inside the QDs. In the second type of structure, the SiGe mixing is suppressed (low growth temperature), and the QDs consist practically of pure Ge. A numerical calculation in the framework of the effective-mass approximation gives $\beta_{SiGe} = 0.0025$ and $\beta_{Ge} = 0.0005$. Taking the *g*-factor value in $Si_{0.3}Ge_{0.7}$ alloy as $g = (1.9995)(0.3) + (2.0412)(0.7) = 2.0287$, we can obtain the *g*-factor change due to the alloy effect equal to $\Delta g \approx 1 \times 10^{-4}$, as observed in the experiments. This value demonstrates that the Ge/Si mixing in our samples does not lead to any significant change of the *g* factor, because the barrier penetration remains very small even after mixing.

E. Anisotropy of electron spin resonance line

The well pronounced anisotropy of the ESR linewidth $\Delta H(\mathbf{H} \perp Z) / \Delta H(\mathbf{H} \parallel Z) \approx 4$ (see Fig. 5) can be explained in terms of an effective magnetic field lying in the plane of the QD array. The origin of this effective field is the structure-induced asymmetry (SIA). In two-dimensional structures, an analog of considered field is the Bychkov-Rashba (BR) field, $H_{BR} = \alpha_{BR}(\mathbf{k} \times \mathbf{n}) / g\mu_B$.[4,15,16] Here, *g* is the electron *g* factor, μ_B is the Bohr magneton, **k** is the in-plane momentum of the electron, and **n** is the unit vector in the growth direction. In QD systems, this field appears during the tunneling between QDs due to the asymmetrical shape of potential wells for electrons. The direction of the tunneling can be considered as an analog to the direction of the electron momentum **k**. Spin

relaxation comes from the precession of the electron spin in the effective magnetic field during certain tunneling events. Such a mechanism of spin relaxation has formerly been considered for the hole hopping transport in QD array.[17]

The tunneling between QDs can be assisted by phonons or by some charge (potential) fluctuations in the Ge QD array.[18] Due to the disorder in QD array, the hopping direction depends on the probability of the tunneling between QDs and can be changed after each tunneling event. As a result, the direction of the effective magnetic field can also be changed. During the tunneling, the spin rotates with the frequency ω_{BR}. The spin phase changes by $\Delta\varphi = \omega_{BR}t$ over time t. Thus, the spin is subjected to a random force that makes the clockwise and anticlockwise spin precessions equally likely, the average spin phase does not change, but the root-mean-square phase change increases with time $(\langle\Delta^2\phi\rangle)^{1/2} = \omega_{BR}\tau_h(t/\tau_h)^{1/2}$, where $1/\tau_h$ is the average rate of hopping between QDs. This consideration is valid for rapid fluctuations (rapid hopping between QDs), $\omega_{BR}\tau_h \ll 1$. A similar case is the spin relaxation in the 2D structures, with replacing the hopping time τ_h by the momentum relaxation time τ_k. In both cases, the phase relaxation time t_ϕ is defined as the time over which the phase fluctuations reach unity: $1/t_\phi = \omega_{BR}^2\tau_h$.

The fluctuating BR field causes the relaxation of a longitudinal spin component with the relaxation time T_1 as well as the relaxation of the transverse spin components with the relaxation time T_2. Assuming that the external magnetic field is applied in the Z direction, the relaxation times are given by[19]

$$\frac{1}{T_1} \sim \delta H_x^2 + \delta H_y^2,$$

$$\frac{1}{T_2} \sim \delta H_z^2 + \frac{1}{2}(\delta H_x^2 + \delta H_y^2),$$

where δH is a fluctuating field. The in-plane components δH_x and δH_y can be associated with the SIA term. The δH_z originates from some background thermal or charge fluctuations, $\delta H_x^2, \delta H_y^2 > \delta H_z^2$, and can be neglected.

Taking the correlation time of the fluctuations τ_c as average hopping time τ_h, the relaxation times can be written as[20]

$$\frac{1}{T_1} = \gamma^2(\delta H_x^2 + \delta H_y^2 \cos^2\theta_H)\frac{\tau_c}{1 + \omega_0^2\tau_c^2},$$

$$\frac{1}{T_2} = \gamma^2\delta H_y^2 \sin^2\theta_H\tau_c + \frac{1}{2T_1}, \qquad (1)$$

where the ω_0 is the Larmor frequency and $\gamma = g\mu_B/\hbar$ is the gyromagnetic ratio.

The width of a homogeneously broadened ESR line at low microwave power is determined by the transverse spin relaxation rate, $1/T_2$. Since the observed ESR line exhibits an inhomogeneous broadening, we can only estimate the lower limit of the spin relaxation time. The linewidth $\Delta H_{pp} = 0.8$ Oe gives the value of $T_2 \sim 10^{-7}$ s.

Let us assume that the inhomogeneous contribution is angle independent, and estimate the magnitude of the BR field based on the experimental angular dependence of the ESR linewidth (Fig. 4). This dependence is well described by the function $\Delta\omega \sim a_1\sin^2\theta_H + a_2\cos^2\theta_H$, where $a_1/a_2 \approx 4$. The last equation allows us to determine the correlation time of the fluctuations. Comparing with Eq. (1), one can write $1 + \omega_0^2\tau_c^2 \approx 4$. Consequently, the correlation time of the fluctuations in our samples is $\tau_c \approx 3 \times 10^{-11}$ s (we take $\omega_0 = 5.89 \times 10^{10}$ s^{-1}). The obtained τ_c corresponds to a reasonable value of the energy overlap integral between closely spaced QDs, $I \sim 10^{-5}$ eV, estimated on the basis of tight-binding calculations[17] for average distance between QDs ($d = 20$ nm). Using the correlation time $\tau_c = 3 \times 10^{-11}$ s and the spin relaxation rate $1/T_2 = 10^7$ s^{-1}, we estimate the magnitude of the BR-like field as $\delta H \approx 30$ Oe. This value is very close to the BR field obtained in ESR experiments on the 2D SiGe structures.[5] The coincidence can be explained by the following considerations. The magnitude of the BR field in the 2D structures depends on the Fermi vector k_F and BR constant α_{BR}, $H_{BR} \sim \alpha_{BR}k_F$. The k_F is determined by the carrier concentration n_s, $k_F \sim \sqrt{n_s}$, with the typical value n_s in the 2D Si/Ge structures being 10^{11} cm^{-2}. In a QD system, the effective magnetic field depends on the height/base ratio of the QD (h/l) (see results of tight-binding calculations[17]). The lateral size of QDs for $n_{QD} = 10^{11}$ cm^{-2} is comparable with the average distance between QDs, $l \sim 1/\sqrt{n_{QD}}$. If the QD height is included in the constant α_{BR} for the QD system, then to ensure the validity of the equality $H_{BR}(QD) = H_{BR}(2D)$, one should assume that the constants α_{BR} for the QD and 2D systems are equal. This assumption will be the subject of our future study.

The tunneling transitions between QDs lead to an important feature observed in the ESR spectra, namely, their narrow linewidth. For localized states, the linewidth is strongly affected by hyperfine fields, in other words, by the electron interactions with the nuclear spins of the isotope ^{29}Si. For donor states in Si, this leads to $\Delta H \approx 2.5$ Oe.[11] In isotopically pure Si, the linewidth goes down to $\Delta H \approx 0.2$ Oe.[11] For 2D electrons, the spatial inhomogeneities of the static field $\mathbf{H}_0$, coming from hyperfine fields, are inhibited by motional narrowing due to the itinerant nature of the electrons. This leads to very narrow linewidths.[5] In our case, the transitions between dots lead to an averaging of the magnetic field inhomogeneity, which, however, is not so effective as in the 2D case. This results in a smaller linewidth than in the case of the donor states in Si, but in a larger one than in the 2D case. We assume that the inhomogeneous broadening of the observed ESR line is a consequence of some incompleteness of the averaging of $\mathbf{H}_0$ deviations in different QDs. In order to distinguish between the homogeneous and inhomogeneous broadening of the ESR line, the spin-echo measurements using appropriate microwave pulse sequences[21] should be done. These experiments will allow us to testify to the validity of our spin relaxation model.

Summarizing, we suggest the following mechanism of the spin relaxation in our samples: the electrons lose their initial spin orientation due to the interaction with an effective magnetic field lying in the plane of the QD array. This magnetic

field arises due to the asymmetry of potential wells for electrons and the fast electron transitions between QDs. Thus, one can assume that in an array of well-separated QDs with negligible charge transitions between them, the proposed mechanism of spin relaxation should be suppressed.

tron transitions between QDs provide the appearance of the Rashba field, the creation of well-separated QD array allows us to preserve the spin orientation for a longer time. The results of these experiments can be used as a basis for direct single-qubit operations with electrons strongly confined in all three dimensions in Si.

IV. CONCLUSIONS

In conclusion, using ESR measurements we have demonstrated the effect of the electron localization in Si in the vicinity of Ge QDs. The obtained values of the parallel and perpendicular g-factor components exactly coincide with $g_\parallel$ and $g_\perp$ in bulk Si, which confirms a top priority of strain in the structures under consideration. The electron spin relaxation time is controlled by the Rashba SO interaction and can increase in more symmetrical structures. As far as the elec-

ACKNOWLEDGMENTS

*aigul@isp.nsc.ru

†Also at 3DFQ UNIFEI, 37500-000 Itajuba, Brazil.

[1] D. Loss and D. P. DiVincenzo, Phys. Rev. A **57**, 120 (1998); B. E. Kane, Nature (London) **393**, 133 (1998).

[2] M. Kroutvar, Y. Ducommun, D. Heiss, M. Bichler, D. Schuh, G. Abstreiter, and J. J. Finley, Nature (London) **432**, 81 (2004).

[3] C. G. Van de Walle, Phys. Rev. B **39**, 1871 (1989).

[4] H. Malissa, W. Jantsch, G. Chen, D. Gruber, H. Lichtenberger, F. Schaffler, Z. Wilamowski, A. M. Tyryshkin, and S. A. Lyon, Mater. Sci. Eng., B **126**, 172 (2006).

[5] Z. Wilamowski, W. Jantsch, H. Malissa, and U. Rössler, Phys. Rev. B **66**, 195315 (2002).

[6] A. I. Yakimov, A. V. Dvurechenskii, A. I. Nikiforov, A. A. Bloshkin, A. V. Nenashev, and V. A. Volodin, Phys. Rev. B **73**, 115333 (2006).

[7] F. Schaffler, Semicond. Sci. Technol. **12**, 1515 (1997).

[8] L. M. Roth, Phys. Rev. **118**, 1534 (1960).

[9] C. G. Van de Walle and R. M. Martin, Phys. Rev. B **34**, 5621 (1986).

[10] A. Dargys and J. Kundrotas, *Handbook on Physical Properties of Ge, Si, GaAs and InP* (Science and Encyclopedia Publishers, Vilnius, 1994).

[11] G. Feher, Phys. Rev. **114**, 1219 (1959).

[12] G. Breit and I. I. Rabi, Phys. Rev. **38**, 2082 (1931).

[13] L. Liu, Phys. Rev. **126**, 1317 (1962).

[14] M. Cardona and F. H. Pollak, Phys. Rev. **142**, 530 (1966).

[15] A. M. Tyryshkin, S. A. Lyon, W. Jantsch, and F. Schäffler, Phys. Rev. Lett. **94**, 126802 (2005).

[16] Y. A. Bychkov and E. I. Rashba, J. Phys. C **17**, 6039 (1984).

[17] A. F. Zinovieva, A. V. Nenashev, and A. V. Dvurechenskii, Phys. Rev. B **71**, 033310 (2005).

[18] A. F. Zinovieva, A. V. Nenashev, and A. V. Dvurechenskii, Proceedings of the 14th International Symposium on Nanostructures: Physics and Technology (Ioffe Institute, St. Petersburg, 2006), p. 363.

[19] Y. Yafet, Solid State Phys. **14**, 1 (1963).

[20] C. P. Slichter, *Principles of Magnetic Resonance* (Springer-Verlag, Berlin, 1978).

[21] A. Schweiger and G. Jeschke, *Principles of Pulse Electron Paramagnetic Resonance* (Oxford University Press, Oxford, 2001).